



## Numerical solution of stochastic models using spectral collocation method

Mehrnoosh Abdous, Alireza Vahidi\*, and Tayebeh Damercheli

Department of Mathematics, Yadegar-e-Imam khomeini (RAH) Share Rey Branch, Islamic Azad University, Tehran, Iran.

### Abstract

In this article, the spectral collocation method based on radial basis functions is used to solve the mentioned models. The advantage of this method is that it converts the equations into a system of algebraic equations. Therefore, we can solve this problem with Newton's method. The purpose of this article is to numerically solve stochastic models such as the Heston model, Vasicek model, Cox-Ingersoll and Ross model and a model of the Black-Scholes called the Genral Stock model. The method is computationally attractive, and numerical examples confirm the validity and efficiency of the proposed method.

**Keywords.** Vasicek model, Cox-Ingersoll and Ross model, Genral stock model, the P panels M-point Newton-Cotes rules, The spectral collocation method based on radial basis functions.

**2010 Mathematics Subject Classification.** 65L05, 34K06, 34K28.

### 1. INTRODUCTION

Valuing and predicting the values of financial options is one of the most challenging topics, which has been particularly attractive to financial specialists, economists, and mathematicians due to the many applications of these contracts in risk hedging. In 1973, Black-Scholes and Merton [2] almost simultaneously introduced the stochastic differential equation that modeled the stochastic behavior of the value of financial assets such as stocks. After the Black-Scholes model, many experts presented models for volatility dynamics to get rid of these defects, including Hall and White [15], Scott [29], Wiggins [34], Stein [30], Melino and Turnbull [23], and Heston [16]. Many experimental studies including Bakshi et al [3] Bailey and Morana [4], and Clark and Devig [6], have shown the superiority of volatility models. Among the stochastic volatility model, the Heston model is one of the most famous stochastic volatility models. Because in this model, asset price volatility is not fixed but follows a random process, so that the asset price process does not accept negative volatility. The Heston model was first introduced in 1993 by Aston Heston.

**1.1. Heston model.** Mathematically, Heston's model assumes that asset prices are determined by a stochastic process. To calculate the underlying price of an asset, the Heston model uses the following equations:

$$dS_t = rS_t dt + \sqrt{V_t} S_t dW_{1t}, \quad (1.1)$$

$$dV_t = K(\theta - V_t) dt + \sigma \sqrt{V_t} dW_{2t}, \quad (1.2)$$

$$dW_{1t} dW_{2t} = \rho dt, \quad (1.3)$$

where  $S_t$  and  $V_t$  are the stock price and variance in time, respectively. In this model, Eqs. (1.1) and (1.2) are called the stock process and the volatility process respectively.

Received: 14 January 2023 ; Accepted: 23 May 2023.  
\*Corresponding author. Email:alrevahidi@yahoo.com .

- $W_{1t}$  is the Brownian motion of the basic asset price.
- $W_{2t}$  is the Browning motion of the variance of the basic asset price.
- $\rho$  is the correlation coefficient between  $W_{1t}$  and  $W_{1t}$ .
- $S_t$  is the price of a particular asset at that time.
- $\sqrt{V_t}$  is the volatility in asset price (a volatility process).
- $\sigma$  is volatility flight.
- $r$  is the risk-free interest rate.
- $\theta$  is the long-term average of volatility process.
- $K$  is the rate-of-return to the long- term price variance (it specifies the speed at which the curves converge around the long-term average).
- $dt$  is the indefinitely small positive time increment.

**1.2. General Stock Model.** Having applied our basic Black-Scholes model to the pricing of some exotic options, we now turn to more general market models. In section we replace the (constant) parameters that characterised our basic Black-Scholes model by previsible processes. Under appropriate boundedness assumptions, to obtain the fair price of an option as the discounted expected value of the claim under a martingale measure. In general this expectation must be evaluated numerically [12]. In the classic Black-Scholes framework, drift is constant and stock volatility is constant. In addition, stock return follows a Brownian motion with a drift constant. In this section, a more general model is considered that can price and hedge derivatives. The key assumption is that there is only one stochastic source in the market and the Brownian motion increases the stock price. By writing  $\{F_t\}_{t \geq 0}$  for the filter that generates the Brownian motion of the stimulus, we replace risk-free loan interest rate  $\{r_t\}$ , drift  $\{\mu_t\}$ , and volatility  $\{\sigma_t\}$  in the basic Black-Scholes model with the predictable processes of  $\{F_t\}_{t \geq 0}$ ,  $\{\mu_t\}_{t \geq 0}$ ,  $\{r_t\}_{t \geq 0}$ ,  $\{\sigma_t\}_{t \geq 0}$ , which can depend on the entire history before the time of  $t$ .

The model consists of a risk-free bond  $\{B_t\}$  and a risky asset of  $\{S_t\}_{t \geq 0}$  that are presented in the following system of equations [12],

$$\begin{cases} dB(t) = r(t)B(t)dt, & B_0 = 1, \\ dS(t) = \mu(t)S(t)dt + \sigma(t)S(t)dW(t), \end{cases} \tag{1.4}$$

or

$$\begin{cases} dB(t) = r(t)B(t)dt, & B_0 = 1, \\ dS(t) = S_0 + \int_0^t \mu(s)S(s)ds + \sigma(s)S(s)dW(s), \end{cases} \tag{1.5}$$

where  $\{W_t\}$  is a P-dimensional Brownian motion that generates the filter of  $\{F_t\}_{t \geq 0}$ , and  $r_t, \mu_t, \sigma_t$  and  $F_t$  are predictable. It is obvious that a solution should be formed for these equations

$$B(t) = \exp\left(\int_0^t r_s ds\right),$$

$$S(t) = S_0 \exp\left(\int_0^t \left(\mu_s - \frac{1}{2}\sigma_s^2\right) ds + \int_0^t \sigma_s ds\right).$$



**1.3. Vasicek model and Cox-Ingersoll-Ross (CIR) model.** As a stochastic investment model and as a single-factor model, the Vasicek model is one of the most recent mathematical models that explains the instantaneous interest rate with changes resulted from only one market risk factor and follows the following stochastic differential equation

$$dr_t = a(b - r_t)dt + \sigma dB_t. \quad (1.6)$$

Since Vasicek allows negative interest rate, Cox-Ingersoll-Ross model can be used to simulate the interest rate.

$$dr = a(b - r)dt + \sigma\sqrt{r}dB, \quad (1.7)$$

$dr$  is the change in the interest rate from one period to another.  $r$  is the current level of interest rate,  $\sigma$  is the annual standard deviation of interest rate,  $dt$  is the time horizon of interest rate calculation. In this problem,  $dB$  is a Wiener random process and  $a$  is the adjustment rate of the long-term average of interest rate  $b$  [20]. Most of these models do not have an analytical solution. Modeling the stock markets usually leads to ordinary and stochastic differential equations. Meshless methods based on radial basis functions are among the methods that have recently attracted the attention because they have the property of spectral convergence, the distribution of points can be arbitrary, and the functions can be approximated. They have been studied by many researchers [13, 14, 18, 24, 31, 32, 35, 36]. Due to the wide application of stochastic equations in various sciences including economics, mechanics, biology, physics, mathematics, and statistics, chemistry, medicine, electronics, etc., and the absence of an exact answer in most cases, the use of numerical methods to solve This group of equations is of considerable importance. Numerical methods or spectral method have already been used in some equations [5, 7, 10, 11, 21, 22, 33]. In this article, the spectral collocation method based on radial basis functions is used as a practical method for solving the models of Heston, General Stock, Vasicek and Cox-Ingersoll-Ross. The proposed method is different from other numerical methods because P-panel M-point Newton-Cotes integration rule was used to estimate the Ito integral in this method. The implementation of this approach can convert the interested problem into a system of algebraic equations that is directly solved by Newton method. The structure of this paper is as follows. In the second section, a number of essential definitions are studied such as Brownian motion, some characteristics of Itos integral, method of radial basis functions, and Newton-Cotes integration rule. In the third section, the numerical solution of the Eqs. (1.1)-(1.2) is presented using the spectral collocation method based on radial basis functions. In the fourth section, the accuracy of the proposed method is investigated by considering numerical examples. Finally, a conclusion is presented in the last section.

## 2. DEFINITIONS AND PERQUISITES

In this section, we overview some definitions and prerequisites that are needed.

**2.1. Some mathematical preliminaries.** Brownian motion [25] is a name that is attributed to the irregular movements of suspended grains in water. It was observed by a Scottish botanist named Robert Brown in 1828. This movement was explained by random collisions with water molecules. For the mathematical definitions of Brownian motion, it is natural to use a stochastic process that is as a position in time. Lets have a mathematical definition of Brownian motion.

**Definition 2.1.** [25]. Suppose  $(\Omega, F, P)$  is a probability space with the filter of  $\{F_t\}_{t \geq 0}$ . A standard one- dimensional Brownian motion with the representation of  $\{B_t\}_{t \geq 0}$  is a real- valued, continuous and  $\{F_t\}$ -adapted process with the following properties:

- 1)  $B_0 = 0$ , almost everywhere.
- 2) For  $0 \leq s < t < \infty$ , the increment of  $B_t - B_s$  is normally distributed with a mean of zero and a variance of  $t - s$ .
- 3) For  $0 \leq s < t < \infty$  the increment of  $B_t - B_s$  is independent of  $F_s^B$ .

Note:  $F_s^B$  is a natural filter.

**Definition 2.2.** [27]. Suppose  $\nu = \nu(T, s)$  is a class of functions  $f(t, w) : [0, \infty] \rightarrow \Omega$  such that



- The function  $(t, w) \rightarrow f(t, w)$  is  $B \times F$ -measurable, where  $B$  is the family of all Borel subsets on  $[0, \infty)$  and  $F$  is the  $\sigma$ -algebra on  $\Omega$ .
- $f(t, w)$  is compatible with  $F_t$ .
- $E[\int_s^T f^2(t, w)dt] < \infty$ .

We show how to define the Ito integral for the Functions of  $f \in \nu$ ,

$$I[f](w) = \int_s^T f(t, w)dB_t(w), \tag{2.1}$$

where  $B_t$  is a one-dimensional Brownian motion.

It is natural to define  $I[\phi]$  for a simple class of functions  $\phi$ . Then we show that each  $f \in \nu$  can be approximated by  $\phi$ 's and we use to define  $\int f dB$  as the limit of  $\int \phi dB$  as  $\phi \rightarrow f$ .

Now we explain the details of this structure. A function of  $\phi \in \nu$  is called elementary if it has the following form.

$$\phi(t, w) = \sum_j e_j(w) \cdot \chi_{[t_j, t_{j+1}]}(t). \tag{2.2}$$

Note that each  $\phi \in \nu$  of the function  $e_j$  must be measurable.

**Definition 2.3.** ([27], (The Ito integral)). suppose  $f \in \nu(S, T) \rightarrow f$ . Then the Ito integral of  $f$  is defined from  $[S, T]$  by

$$\int_s^T f(t, w)dB_t = \lim_{m \rightarrow \infty} \int_s^T \varphi_n(t, w)dB_t(w), \quad (\text{lim in } L^2(P)), \tag{2.3}$$

where,  $\varphi_n$  is a sequence of elementary functions such that

$$E[\int_s^T (f(t, w) - \varphi_n(t, w))^2 dt] \rightarrow 0, \quad n \rightarrow \infty. \tag{2.4}$$

**Property 1 ([27], Integration by parts):** Suppose  $f(s, w) = f(s)$  only depends on  $s$  and  $f$ . It is continuous and bounded on the interval  $[0, t]$ . Then

$$\int_0^t f(s)dB_s = f(t)B_t - \int_0^t B_s df_s. \tag{2.5}$$

**Property 2 (The Itô isometry):** Suppose  $f \in \nu(S, T)$

$$E[(\int_s^T f(t, w)dB_t(w))^2] = E[\int_s^T f^2(t, w)dt]. \tag{2.6}$$

*Proof.* see ([27], p.26). □

## 2.2. Radial basis functions.

2.2.1. *Definition of radial basis functions.* Here we present an introduction to RBF theory. Let  $R^+ = \{x \in R, x \geq 0\}$  be a non-negative half-line and Let  $\phi : R^+ \rightarrow R$  be a continuous function with  $\phi(0) \geq 0$ . The radial basis function on  $R^d$  has the following form.

$$\phi(\|x - x_i\|),$$



TABLE 1. Classification of standard radial basis functions.

classic shape	symbol	The name of the radial basis function	grouping
$\sqrt{r^2 + c^2}$	MQ	Multiquadric	Continuously smooth
$\frac{1}{\sqrt{r^2 + c^2}}$	IMQ	Inverse Multiquadric	
$e^{-(cr)^2}$	GA	Gaussian	
$r$	LN	Linear	Piecewise smooth
$r^3$	CU	Cubic	
$r^2 \ln(r)$	TPS	Thin Plate Spline	

where  $X, X_i \in R^d$  and  $\|\cdot\|$  are the Euclidean norm between  $X$  and  $X_i$ . In addition, Euclidean norm is the most choice for the norm of  $\|\cdot\|$ , that is, the norm of  $L^2$ . If  $N$  points of  $\{X_i\}_{i=1}^N$  are selected in  $R^d$ , then

$$y(x) = \sum_{i=1}^N \alpha_i \phi(\|X - X_i\|), \quad \lambda_i \in R, \quad (2.7)$$

is called a radial basis function.

**2.2.2. RBF interpolation.** The one-dimensional function of  $y(x)$  is approximated or interpolated, which can be represented by an RBF in the following form:

$$y(x) \approx y_N(x) = \sum_{i=1}^N \alpha_i \phi(\|x\|), \quad x \in R^d. \quad (2.8)$$

$X$  is the interpolation points, and  $\{\alpha_i\}_{i=1}^N$  is a coefficient that must be determined [1]. By choosing  $N$  interpolation point  $\{X_i\}_{i=1}^N$ , the approximate function can be written as follows:

$$y_j = \sum_{i=1}^N \alpha_i \phi_i(x_j), \quad j = 1, 2, \dots, N. \quad (2.9)$$

Standard radial basis function can be classified into two important groups [19]. The first group is infinitely smooth radial basis functions [8, 19]. These basis functions are infinitely differentiable and strongly depend on the shape parameter, for example, the multiquadric function, the Gaussian function, etc (see Table 1). The second group are infinitely smooth functions (except in the centers). Basic functions are not very different from this group. These basic functions are without shape parameter and have relatively less accuracy than the basic functions discussed in the first group.

### 2.3. A summary of the integration rule of the Newton-Cotes method. [9].

The integration rule is the basic of any numerical method for solving integral equations. The integration rule is a general name given to any numerical method for evaluating the approximation of an integral of a function  $f(x)$

$$If = \int_a^b w(s)f(s)ds, \quad (2.10)$$

where  $w(s)$  is a weight function that can use any information contained in the function  $f(s)$  such as the values of its derivatives one or more points and values of simpler integral. We only consider the cases in which the used information is restricted to the value in a set of points  $\{\xi_i, i = 1, \dots, N\}$  and the approximation (integration rule) has the forms as follows,

$$Qf = \sum_{i=1}^N w_i f(\xi_i) = If - Ef. \quad (2.11)$$



$Ef$  is the error.

Newton-Cotes integral quadrature rule ( $Q_M$ ) are obtained by integrating of polynomial uniformly spaced interpolants of the integrand. The  $M$ -point Newton-Cotes rule ( $M \geq 2$ ) is defined by

$$Q_M f(a, b) = \int_a^b q_{m-1}(x) dx, \tag{2.12}$$

where  $q_{m-1}(x)$  interpolates function  $f(x)$  in the following points.

$$x_i = a + \frac{i-1}{M-1}(b-a), \quad i = 1, 2, \dots, M. \tag{2.13}$$

The error  $|If - Q_M f|$  may not converge to zero, even for well-behavior functions of  $f$ . So, we obtain  $P$ -panel  $Q_M$  rule approximation to the integral  $\int_a^b f(s) ds$  by setting  $h = \frac{b-a}{M}$ . In general, the method includes dividing the interval of  $[a, b]$  into sub-interval of  $T_j = [a + (j-1)h, a + jh], j = 1, 2, \dots, P$ . So, we use the interpolation formula in each sub-interval with the points of  $\{X_i^{(j)}\}_{i=1}^M$  and the weight of  $\{w_i^{(j)}\}_{i=1}^M, j = 1, \dots, P$ .

$$\begin{aligned} If &= \int_a^b f(s) ds = \sum_{j=1}^P \int_{a+(j-1)h}^{a+jh} f(s) ds \\ &= \sum_{j=1}^P Q_M(a + (j-1)h, a + jh) f + E_M \\ &= \sum_{j=1}^P \sum_{i=1}^M w_k^{(j)}(f(x_k^{(j)})) + E_{M,P}. \end{aligned} \tag{2.14}$$

for fixed  $M$  and increasing  $P$  these also yield a sequence of approximation to  $If$ .

**Property 3.[9]:** With notation as in (2.14), is as follows for every fixed  $M$  and for every  $(a, b)$ -Riemanns integrable function  $f$ :

$$\lim_{m \rightarrow \infty} E_{M,P} = 0. \tag{2.15}$$

### 3. NUMERICAL SOLUTION

The proposed method can be applied to each of four models of Heston, General Stock, Vasicek, and Cox-Ingersoll-Ross, since Hestons model is more general, we implemented the method on the Hestons model. Here, we consider the Heston model and expand  $s_N(t)$  and  $v_N(t)$  as follows

$$s_t = s_0 + r \int_0^t s_t(s) ds + \int_0^t \sqrt{v_t(s)} s_t(s) dW_1(s), \tag{3.1}$$

$$v_t = v_0 + k \int_0^t (\theta - v_t(s)) ds + \sigma \int_0^t \sqrt{v_t(s)} dW_2(s), \tag{3.2}$$

$$S(t) \simeq s_N(t) = \sum_0^N \alpha_i \phi_i(t), \tag{3.3}$$

$$v(t) \simeq v_N(t) = \sum_0^N \alpha'_i \phi_i(t). \tag{3.4}$$

By substituting two Eqs. (3.3)-(3.4) in Eqs. (3.1)-(3.2), we have:

$$s_N(t) = s_0 + r \int_0^t s_N(s) ds + \int_0^t \sqrt{v_N(s)} s_N(s) dW_1(s) + Res_N(t), \tag{3.5}$$



$$v_N(t) = v_0 + k \int_0^t (\theta - v_N(s)) ds + \sigma \int_0^t \sqrt{v_N(s)} dW_2(s) + Res_N(t), \quad (3.6)$$

where  $Res_N(t)$  is the residual error when  $t \in [0, 1]$ . This error is generated when substitution takes place in the equations to solve the approximation. Using the integral by parts (property 1), we have the following results

$$\int_0^t \sqrt{v_N(s)} s_N(s) dW_1(s) = \sqrt{v_N(t)} s_N(t) W_1(t) - \int_0^t W_1(s) (\sqrt{v_N(s)} s_N(s))' ds, \quad (3.7)$$

$$\int_0^t \sqrt{v_N(s)} dW_2(s) = \sqrt{v_N(t)} W_2(t) - \int_0^t W_2(s) (\sqrt{v_N(s)})' ds, \quad (3.8)$$

to solve the second integral in Eqs. (3.7)-(3.8), we use the Newton-Cotes rule as follows. We convert the interval of the integral into the fixed interval of  $[0, 1]$ .

$$s = tx, \quad x \in [0, 1], \quad s \in [0, t].$$

$$s_N(t) = s_0 + rt \int_0^1 s_N(tx) dx + t(\sqrt{v_N(t)} s_N(t) W_1(t) - \int_0^1 (\sqrt{v_N(tx)} s_N(tx))' W_1(tx) dx) + Res_N(t), \quad (3.9)$$

$$v_N(t) = v_0 + kt \int_0^1 (\theta - v_N(tx)) dx + \sigma t (\sqrt{v_N(t)} W_2(t) - \int_0^1 (\sqrt{v_N(tx)})' W_2(tx) dx) + Res_N(t), \quad (3.10)$$

then Eqs. (3.9)-(3.10) are approximated using  $P$ -panel  $M$ -point Newton-Cotes integration rule as follows:

$$s_N(t) = s_0 + \sqrt{v_N(t)} s_N(t) W_1(t) + t \sum_{j=1}^P \sum_{i=1}^M w_i^{(j)} [r s_N(tx_i^{(j)}) - (\sqrt{v_N(tx_i^{(j)})} s_N(tx_i^{(j)}))' w_1(tx_i^{(j)})] + E_{M,P} + Res_N(t), \quad (3.11)$$

$$v_N(t) = v_0 + \sqrt{v_N(t)} W_2(t) + t \sum_{j=1}^P \sum_{i=1}^M [k(\theta - v_N(tx_i^{(j)})) - \sigma (\sqrt{v_N(tx_i^{(j)})})' w_2(tx_i^{(j)})] + E_{M,P} + Res_N(t), \quad (3.12)$$

where  $\{x_i^j\}_{i=1}^M, \{w_i^j\}_{i=1}^M, j = 1, \dots, P$  are Newton-Cotes points and weights respectively [28].  $E_{M,P}$  is the error of numerical integration. Now by replacing the collocated points  $t_l$  in Eqs. (3.11)-(3.12), it becomes a system of algebraic equation. By solving it, we get the approximate solution of  $s_N(t)$  and  $v_N(t)$ .

$$s_N(t_l) = s_0 + \sqrt{v_N(t_l)} s_N(t_l) W_1(t_l) + t_l \sum_{j=1}^P \sum_{i=1}^M w_i^{(j)} [r s_N(t_l x_i^{(j)}) - (\sqrt{v_N(t_l x_i^{(j)})} s_N(t_l x_i^{(j)}))' w_1(t_l x_i^{(j)})], \quad (3.13)$$

$$v_N(t_l) = v_0 + \sqrt{v_N(t_l)} W_2(t_l) + t_l \sum_{j=1}^P \sum_{i=1}^M [k(\theta - v_N(t_l x_i^{(j)})) - \sigma (\sqrt{v_N(t_l x_i^{(j)})})' w_2(t_l x_i^{(j)})], \quad (3.14)$$

a set of collocated points is considered as the equidistant point.  $a$  is the beginning of the interval and  $h$  is the step length

$$t_l = a + lh, \quad l = 0, 1, \dots, N.$$



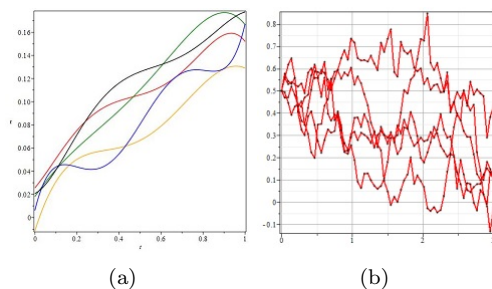


FIGURE 1. The graph of the approximate solutions of Example 4.1 based on the proposed method (left) and the graph of the block pulse method [17] (right).

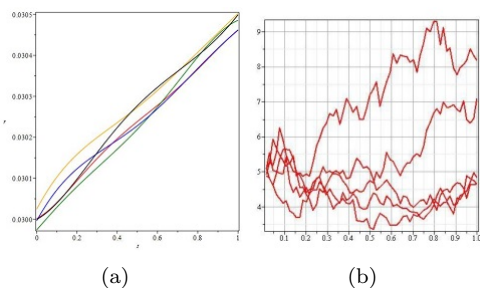


FIGURE 2. The graph of the approximate solutions of Example 4.2 based on the proposed method (left) and the graph of the block pulse method [17] (right).

#### 4. NUMERICAL EXAMPLES

In this section, some numerical examples are presented to confirm the efficiency and accuracy of the proposed method. All computations were conducted using Maple software (2019) on a laptop with the following characteristics: 4 GB RAM, 2.10 GHz core i3, Intel (R), Pentium (R).

**Example 4.1.** Here, we consider Eq. (1.6) and determine the initial values and parameters as  $\sigma = 0.3, b = 0.25, a = 1, r = 0.03$ . In the article[17], the same example is solved with the given values. In Figure 1, we show five paths of the approximate solutions of Vasicek model based on the proposed method (left) and the graph solutions of the mentioned model based on the block pulse method (right).

**Example 4.2.** multiple paths of the solution of Cox-Ingersoll-Ross Eq. (1.7) are shown in Figure 2 with the following initial values and parameters,  $\sigma = 0.002, b = 0.04, a = 0.05, r = 0.03$ (left). The same example is solved in the article [17], with the given values based on the block pulse method, five paths shown in Figure 2 (right).

**Example 4.3.** Here, the Heston model of Eqs. (1.1)-(1.2) is considered with the initial conditions of  $S_0 = 0.5$  and  $V_0 = 0.5$  The parameters are selected as  $\theta = 0.1, r = 0.05, k = 1, \sigma = 0.1$ . Five paths of approximate solutions for  $S_t$  and  $V_t$  are plotted in Figure 3 using spectral collocation method based on radial basis functions (left) and The same example is solved in the article [17] , with the given values based on the block pulse method, five paths for  $S_t$  and  $V_t$  shown in Figure 3 (right).

**Example 4.4.** Consider the following general stock model [26]:

$$\begin{cases} dB(t) = \sin(t)B(t)dt, & B_0 = 1, \\ S(t) = \frac{1}{10} + \int_0^t \ln(1+s)S(s)ds + \int_0^t sS(s)dW(S) & s, t \in [0, 0.8), \end{cases}$$





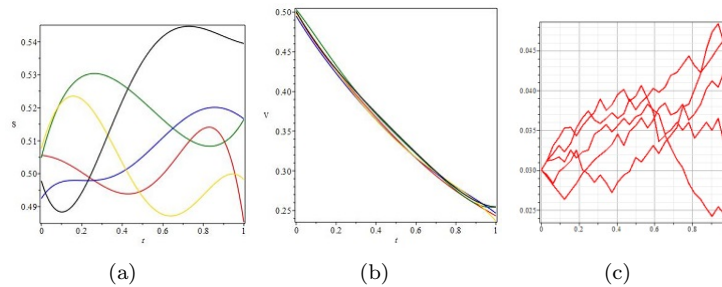


FIGURE 3. The graph of the approximate solutions of Example 4.3 based on the proposed method (left) and the graph of the block pulse method [17] (right).

TABLE 2. The absolute error of spectral collocation method based on radial basis functions with  $\varphi(r) = \sqrt{r^2 + c^2}$  for different  $N$ .

$t$	$N = 2^2$	$N = 2^3$	$N = 2^4$	$N = 2^5$	$N = 2^6$	$N = 80$
0	0	0	0	0	0	$2.10 \times 10^{-10}$
0.1	$7.47 \times 10^{-5}$	$1.26 \times 10^{-4}$	$4.47 \times 10^{-5}$	$1.81 \times 10^{-6}$	$3.71 \times 10^{-8}$	$2.09 \times 10^{-9}$
0.2	$1.41 \times 10^{-4}$	$1.31 \times 10^{-4}$	$9.98 \times 10^{-6}$	$2.27 \times 10^{-6}$	$4.34 \times 10^{-8}$	$1.90 \times 10^{-9}$
0.3	$3.65 \times 10^{-4}$	$1.15 \times 10^{-6}$	$9.73 \times 10^{-6}$	$2.35 \times 10^{-6}$	$5.76 \times 10^{-8}$	$1.40 \times 10^{-9}$
0.4	$5.92 \times 10^{-4}$	$7.12 \times 10^{-5}$	$2.21 \times 10^{-5}$	$7.69 \times 10^{-7}$	$1.77 \times 10^{-7}$	$1.00 \times 10^{-10}$
0.5	$3.20 \times 10^{-5}$	$5.99 \times 10^{-6}$	$7.87 \times 10^{-7}$	$4.82 \times 10^{-8}$	$1.68 \times 10^{-8}$	$2.27 \times 10^{-8}$
0.6	$6.74 \times 10^{-4}$	$7.61 \times 10^{-5}$	$2.04 \times 10^{-5}$	$2.88 \times 10^{-7}$	$1.62 \times 10^{-6}$	$7.00 \times 10^{-10}$
0.7	$4.87 \times 10^{-4}$	$1.67 \times 10^{-4}$	$1.30 \times 10^{-5}$	$1.47 \times 10^{-6}$	$2.80 \times 10^{-6}$	$4.49 \times 10^{-8}$
0.8	$4.42 \times 10^{-4}$	$1.76 \times 10^{-4}$	$1.43 \times 10^{-5}$	$1.21 \times 10^{-6}$	$1.04 \times 10^{-6}$	$2.39 \times 10^{-7}$
cpu time(s)	39.57	39.45	40.51	44.08	52.89	59.46

with the exact solution of  $B(t) = e^{1-\cos(t)}$ ,  $S(t) = \frac{1}{10}e^{(1+t)\ln(1+t)-t-\frac{t^3}{6}+\int_0^t sdW(s)}$  for  $t \in [0, 0.8]$ . The spectral collocation method was presented in section 3 to solve General Stock model numerically. Note that  $N$  is the number of collocation points,  $P$  is the number of sub-intervals and  $M$  is the number of points ( $M = 4, P = 10, c = 0.01$ ). Tables 2, 3, and 4 show the error of the presented method in section 3 for different values of  $N$  in the interval of  $[0, 0.8]$  and Gaussian, cubic and multiquadric radial basis functions. In addition, average error of this method is obtained for all three basis functions and different values of  $N$ . Then it is compared with that of block pulse functions [26]. The results are presented in Tables 5, 6, and 7. The results show that more exact approximations are obtained by increasing the  $N$ . The results were compared with those reported in [26] that indicated the accuracy and efficiency of the presented method. Numerical results have an acceptable accuracy with small  $N$ , and better accuracy can be obtained by increasing the  $N$ . Also, the reported cpu times show that the collocation spectral method based on the radial basis functions is fast and easy to implement.

**Note 1:** The concept of Block pulse functions was first introduced by Harmuth in the field of electrical engineering. Then it was used by many researchers in different fields. One of the objectives of using Block pulse functions is to find an appropriate approximation for solving differential and integro-differential equations. So, we introduce Block pulse functions, their characteristics and the related operational matrix in [26]. An  $m$ -tuple set of Block pulse functions on the interval  $[0, T]$  is defined as follows

$$\varphi_i = \begin{cases} 1, & (i-1)h \leq t < ih, \quad i = 1, 2, \dots, m, h = \frac{T}{m}, \\ 0, & o.w, \end{cases}$$



TABLE 3. The absolute error of spectral collocation method based on radial basis functions with  $\varphi(r) = r^3$  for different  $N$ .

$t$	$N = 2^2$	$N = 2^3$	$N = 2^4$	$N = 2^5$	$N = 2^6$	$N = 80$
0	0	0	0	$2.10 \times 10^{-3}$	0	$1.99 \times 10^{-2}$
0.1	$1.52 \times 10^{-3}$	$5.15 \times 10^{-4}$	$2.15 \times 10^{-4}$	$4.85 \times 10^{-4}$	$4.85 \times 10^{-4}$	$2.29 \times 10^{-2}$
0.2	$2.07 \times 10^{-4}$	$8.93 \times 10^{-4}$	$4.07 \times 10^{-4}$	$1.79 \times 10^{-3}$	$1.19 \times 10^{-2}$	$2.55 \times 10^{-2}$
0.3	$3.10 \times 10^{-4}$	$4.90 \times 10^{-4}$	$1.02 \times 10^{-5}$	$6.90 \times 10^{-4}$	$5.81 \times 10^{-3}$	$2.28 \times 10^{-3}$
0.4	$3.36 \times 10^{-4}$	$2.64 \times 10^{-4}$	$1.76 \times 10^{-4}$	$5.34 \times 10^{-4}$	$2.64 \times 10^{-3}$	$5.62 \times 10^{-3}$
0.5	$3.62 \times 10^{-4}$	$2.38 \times 10^{-4}$	$9.78 \times 10^{-5}$	$1.48 \times 10^{-4}$	$5.62 \times 10^{-4}$	$1.76 \times 10^{-3}$
0.6	$5.17 \times 10^{-4}$	$1.83 \times 10^{-4}$	$2.34 \times 10^{-4}$	$1.41 \times 10^{-4}$	$1.62 \times 10^{-3}$	$5.90 \times 10^{-3}$
0.7	$8.18 \times 10^{-4}$	$1.32 \times 10^{-4}$	$2.92 \times 10^{-4}$	$3.93 \times 10^{-4}$	$5.73 \times 10^{-4}$	$7.75 \times 10^{-3}$
0.8	$1.01 \times 10^{-3}$	$2.36 \times 10^{-4}$	$3.89 \times 10^{-4}$	$8.70 \times 10^{-4}$	$1.86 \times 10^{-2}$	$3.73 \times 10^{-3}$
cpu time(s)	39.57	39.45	40.07	42.04	46.25	52.54

TABLE 4. The absolute error of spectral collocation method based on radial basis functions with  $\varphi(r) = e^{-(cr)^2}$  for different  $N$ .

$t$	$N = 2^2$	$N = 2^3$	$N = 2^4$	$N = 2^5$	$N = 2^6$	$N = 80$
0	0	$5.10 \times 10^{-3}$	$2.00 \times 10^{-3}$	$1.08 \times 10^{-2}$	$3.00 \times 10^{-2}$	$6.00 \times 10^{-4}$
0.1	$5.15 \times 10^{-4}$	$4.51 \times 10^{-3}$	$1.25 \times 10^{-2}$	$1.22 \times 10^{-2}$	$9.52 \times 10^{-2}$	$3.42 \times 10^{-3}$
0.2	$1.11 \times 10^{-3}$	$9.29 \times 10^{-3}$	$5.11 \times 10^{-3}$	$5.41 \times 10^{-3}$	$2.19 \times 10^{-2}$	$2.11 \times 10^{-3}$
0.3	$8.10 \times 10^{-4}$	$3.61 \times 10^{-3}$	$1.88 \times 10^{-2}$	$5.01 \times 10^{-3}$	$1.41 \times 10^{-3}$	$1.27 \times 10^{-3}$
0.4	$6.36 \times 10^{-4}$	$3.04 \times 10^{-3}$	$4.64 \times 10^{-3}$	$8.74 \times 10^{-3}$	$2.26 \times 10^{-2}$	$5.67 \times 10^{-4}$
0.5	$4.38 \times 10^{-4}$	$9.38 \times 10^{-4}$	$5.62 \times 10^{-4}$	$1.26 \times 10^{-2}$	$4.14 \times 10^{-2}$	$4.27 \times 10^{-4}$
0.6	$3.83 \times 10^{-4}$	$8.58 \times 10^{-3}$	$1.56 \times 10^{-2}$	$5.17 \times 10^{-4}$	$1.64 \times 10^{-2}$	$3.21 \times 10^{-4}$
0.7	$1.27 \times 10^{-34}$	$1.02 \times 10^{-2}$	$7.28 \times 10^{-4}$	$1.45 \times 10^{-2}$	$2.27 \times 10^{-3}$	$7.88 \times 10^{-4}$
0.8	$2.39 \times 10^{-3}$	$5.10 \times 10^{-3}$	$3.70 \times 10^{-3}$	$1.13 \times 10^{-2}$	$3.39 \times 10^{-2}$	$1.28 \times 10^{-3}$
cpu time(s)	39.43	39.63	40.56	44.80	56.23	66.23

TABLE 5. Comparison of absolute error of Block pulse method [26] and approach of Example 4.4.

N	Block-pulse method[26]	our approach $\varphi(r) = \sqrt{r^2 + c^2}$
4	$1.50 \times 10^{-2}$	$2.82 \times 10^{-4}$
8	$2.60 \times 10^{-2}$	$3.19 \times 10^{-4}$
16	$3.56 \times 10^{-2}$	$4.70 \times 10^{-5}$
32	$5.52 \times 10^{-2}$	$5.99 \times 10^{-6}$
64	$9.67 \times 10^{-2}$	$4.70 \times 10^{-7}$
80	$1.12 \times 10^{-1}$	$1.51 \times 10^{-7}$

TABLE 6. Comparison of absolute error of Block pulse method [26] and approach of Example 4.4.

N	Block-pulse method[26]	our approach $\varphi(r) = r^3$
4	$1.50 \times 10^{-2}$	$7.50 \times 10^{-4}$
8	$2.60 \times 10^{-2}$	$1.26 \times 10^{-3}$
16	$3.56 \times 10^{-2}$	$3.48 \times 10^{-4}$
32	$5.52 \times 10^{-2}$	$2.55 \times 10^{-4}$
64	$9.67 \times 10^{-2}$	$1.03 \times 10^{-2}$
80	$1.12 \times 10^{-1}$	$4.27 \times 10^{-3}$



TABLE 7. Comparison of absolute error of Block pulse method [26] and approach of Example 4.4.

N	Block-pulse method[26]	our approach $\varphi(r) = e^{-(cr)^2}$
4	$1.50 \times 10^{-2}$	$2.55 \times 10^{-4}$
8	$2.60 \times 10^{-2}$	$8.89 \times 10^{-3}$
16	$3.56 \times 10^{-2}$	$4.27 \times 10^{-3}$
32	$5.52 \times 10^{-2}$	$2.66 \times 10^{-3}$
64	$9.67 \times 10^{-2}$	$1.03 \times 10^{-2}$
80	$1.12 \times 10^{-1}$	$2.51 \times 10^{-1}$

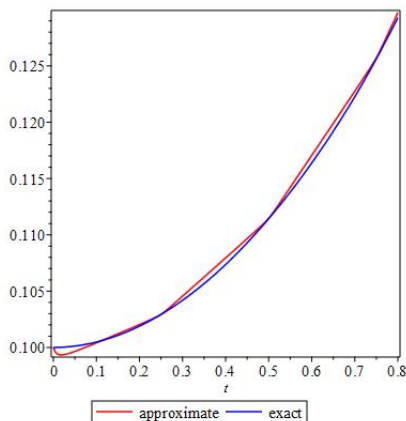


FIGURE 4. The graph of the approximate and exact solution of Example 4.4 with function  $\varphi(r) = \sqrt{r^2 + c^2}$  and  $N=12$ .

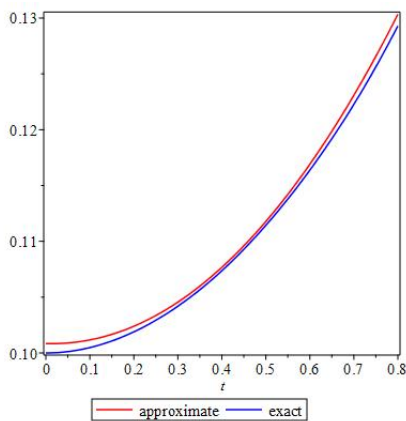


FIGURE 5. The graph of the approximate and exact solution of Example 4.4 with function  $\varphi(r) = r^3$  and  $N=12$ .

### 5. CONCLUSION

In this paper, an efficient and attractive computational method was presented for the numerical solution of Heston, Vasicek, Cox-Ingersoll-Ross, and General Stock models. The spectral collocation method based on radial basis functions was used to numerically solve these models. A number of examples were presented in this paper to verify



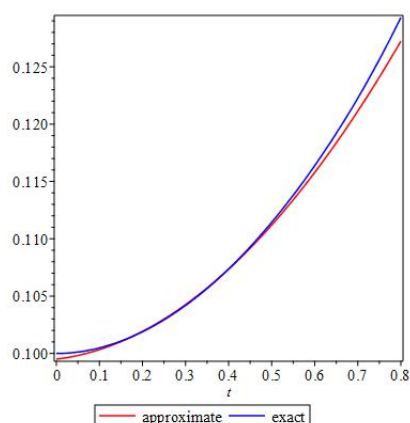


FIGURE 6. The graph of the approximate and exact solution of Example 4.4 with function  $\varphi(r) = e^{-(cr)^2}$  and  $N=12$ .

the reliability and efficiency of the presented method. Furthermore, The graph of approximate and exact solution for  $N = 12$  and Gaussian, cubic and multiquadric radial basis functions are illustrated in Figures 4, 5, and 6 The results showed that the proposed method is easy to implement and is a powerful tool to numerically solve the stochastic differential equations including the models mentioned in this paper. The presented graphs showed that it is easy to implement the proposed method. In addition, the comparisons made in Example 4.4 showed that the proposed method is better for multiquadric and cubic functions.

#### REFERENCES

- [1] A. Alipanah and M. Dehghan, *Numerical solution of the nonlinear Fredholm integral equations by positive definite functions*, Appl. Math. Comput., 190 (2007), 1754-1761.
- [2] F. Black and M. Sholes, *The Pricing of Options and Corporate Liabilities*, Journal of Political Economy, 81 (1973), 637-654.
- [3] G. Bakshi, C. Cao, and Z. Chen, *Empirical performance of alternative option pricing models*, The Journal of Finance, 52(5) (1990), 2003-2049.
- [4] R. T. Baillie and C. Morana, *Modelling long memory and structural breaks in conditional variances: An adaptive FIGARCH approach*, Journal of Economic Dynamics and Control, 33(8) (2009), 1577-1992.
- [5] A. Babaei, H. Jafari, S. Banihashemi, and M. Ahmadi, *A Stochastic Mathematical Model for COVID-19 According to Different Age Groups*, Applied and computational mathematics, 20(1) (2021), 140-159.
- [6] T. E. Clark and T. Davig, *Decomposing the declining volatility of long-term inflation expectations*, Journal of Economic Dynamics and Control, 35(7) (2011), 981-999.
- [7] S. R. Chakravarthy and ö. erife, *Analysis of a Stochastic Model for Crowdsourcing Using Map Arrivals and Phase Type Services*, Applied and computational mathematics, 20(3) (2021), 390-407.
- [8] M. Dehghan and A. Shokri, *A meshless method for numerical solution of the one-dimensional wave equation with an integral condition using radial basis functions*, Numer. Algor., 52 (2009), 461-477.
- [9] L. M. DELVES and J. L. MOHAMED, *Computational methods for integral equations*, Departement of Statistics and Computational Mathematics, University of Liverpool, Cambridge University Press (1985), 23-28.
- [10] M. R. Doostdar, A. R. Vahidi, T. Damercheli, and E. Babolian, *A numerical method based on hybrid functions for solving a fractional model of HIV infection of CD4+ T cells*, Mathematical Sciences, (2022), 1 -11.
- [11] M. R. Doostdar, A. R. Vahidi, T. Damercheli, and E. Babolian, *A hybrid functions method for solving linear and non-linear systems of ordinary differential equations*, Mathematical Communications, 26(2) (2021), 197-213.
- [12] A. Etheridge, *A Course in Financial Calculus*, Cambridge University Press, (2002).
- [13] R. Frank, *Scattered data interpolation: tests of some methods*, Math. Comput, 38 (1982), 181-199.



- [14] G. E. Fasshauer, *Solving differential equations with radial basis functions: multi-level methods and smoothing*, Adv.in Comp.Math., 11 (1999), 139-159.
- [15] J. Hull and A. White, *The pricing of options on assets with stochastic volatilities*, 42(2) (1987), 281-300.
- [16] S. L. Heston, *A closed-form solution for options with stochastic volatility with applications to bond and currency options*, Review of Financial Studies, 6(2) (1993), 327-343.
- [17] F. Hossieni Shekarabi and T. Damercheli, *Application of operational matrices in numerical solution of stochastic differential equations in financial mathematics*, 4th Seminar of Mathematics and Humanities (Financial Mathematics), (2016), 81-85.
- [18] S. Islam, S. Haq, and A. Ali, *A meshfree method for the numerical solution of the RLW equation*, Journal of Computational and Applied Mathematics, 223 (2009), 997-1012.
- [19] A. J. Khattak, S. I. A. Tirmizi, and S.U. Islam, *Application of meshfree collocation method to a class of nonlinear partial differential equations*, Eng. Anal. Bound. Elem., 33 (2009), 661-667.
- [20] F. C. Klebaner, *Introduction to Stochastic Calculus with Applications*, Imperial College Press, London, (2005).
- [21] M. Kazemi, A. Deep, and A. Yaghoobnia, *Application of fixed point theorem on the study of the existence of solutions in some fractional stochastic functional integral equations*, Mathematical Sciences, (2022), 1-12.
- [22] M. Kazemi and A. R. Yaghoobnia, *Application of fixed point theorem to solvability of functional stochastic integral equations*, Applied Mathematics and Computation, 417 (2022), 126759.
- [23] A. Melino and S. Turnbull, *Pricing foreign currency options with stochastic volatility*, Journal of Econometrics, 45 (1990), 239-265.
- [24] C. Micchelli, *Interpolation of scattered data: distance matrices and conditionally positive definite functions*, Constructive Approximation, 2 (1986), 11-22.
- [25] X. Mao, *Stochastic Differential Equation and Application Second Edition*, Departement of Statistics and Modelling Science, University of Strathclyde, Glasgow, (2007).
- [26] K. Maleknejad, M. Khodabin, and M. Rostami, *Numerical solution of stochastic Volterra integral equations by a stochastic operational matrix based on block pulse functions*, Math. Comput. Model, 55 (2012), 791-800.
- [27] B. Oksendal, *Stochastic Differential Equations An Introduction with Applications*, Fifth Edition Corrected Printing Springer-Verlag Heidelberg New York, May, 2014.
- [28] G. M. Phillips and P. J. Taylor, *Theory and Application of Numerical Analysis*, Academic Press, New York, 1973.
- [29] L. O. Scott, *Option pricing when the variance changes randomly: Theory, estimation, and an application*, Journal of Financial Economics, 22(4) (1987), 419-438.
- [30] E. M. Stein and J. C. Stein, *Stock price distributions with stochastic volatility: an analytic approach*, The Review of Financial Studies, 4(4) (1991), 727-752.
- [31] R. Schaback, *Error Estimates and Condition Numbers for Radial Basis Function Interpolation*, Advances in Computational Mathematics, 3 (1995), 251-264.
- [32] M. Shiralizadeh, A. Alipanah, and M. Mohammadi, *A numerical method for KdV equation using rational radial basis functions*, Computational Methods for Differential Equations, 2 (2023), 303-318.
- [33] A. R. Vahidi, E. Babolian, and Z. Azimzadeh, *An Improvement to the Homotopy Perturbation Method for Solving Nonlinear Duffings Equations*, Bulletin of the Malaysian Mathematical Sciences Society, 41 (2018), 1105-1117.
- [34] J. B. Wiggins, *Option values under stochastic volatility: Theory and empirical estimates*, Journal of Financial Economics, 19(2) (1987), 351-372.
- [35] H. Wendland, *Piecewise polynomial, positive definite and compactly supported radial functions of minimal degree*, Advances in Computational Mathematics, 4 (1995), 389-396.
- [36] M. R. Yaghoti and F. Farshadmoghadam, *Choosing the best value of shape parameter in radial basis functions by Leave-P-Out Cross Validation*, Computational Methods for Differential Equations, 1 (2023), 108-129.

